

Monodisperse Polymeric Ionic Liquid Microgel Beads with Multiple Chemically Switchable Functionalities

Md. Taifur Rahman,^{§,⊥} Zahra Barikbin,^{†,⊥} Abu Zayed M. Badruddoza,[‡] Patrick S. Doyle,^{†,||} and Saif A. Khan^{*,†,‡}

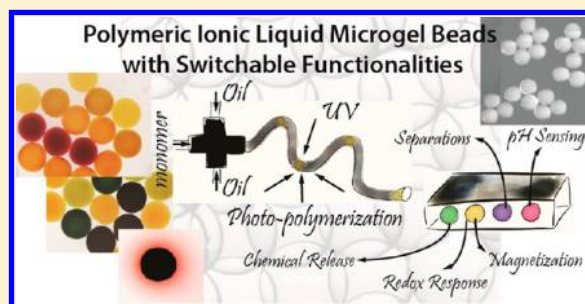
[†]Singapore-MIT Alliance and [‡]Department of Chemical and Biomolecular Engineering, National University of Singapore, 4 Engineering Drive 3, 117576, Singapore

[§]School of Chemistry and Chemical Engineering, The Queen's University of Belfast, Belfast, BT9 5AG, United Kingdom

^{||}Department of Chemical Engineering, Massachusetts Institute of Technology, 77 Massachusetts Avenue, Cambridge, Massachusetts 02139, United States

S Supporting Information

ABSTRACT: We present simple, inexpensive microfluidics-based fabrication of highly monodisperse poly(ionic liquid) microgel beads with a multitude of functionalities that can be chemically switched in facile fashion by anion exchange and further enhanced by molecular inclusion. Specifically, we show how the exquisite control over bead size and shape enables extremely precise, quantitative measurements of anion- and solvent-induced volume transitions in these materials, a crucial feature driving several important applications. Next, by exchanging diverse anions into the synthesized microgel beads, we demonstrate stimuli responsiveness and a multitude of novel functionalities including redox response, controlled release of chemical payloads, magnetization, toxic metal removal from water, and robust, reversible pH sensing. These chemically switchable stimulus-responsive beads are envisioned to open up a vast array of potential applications in portable and preparative chemical analysis, separations and spatially addressed sensing.



INTRODUCTION

Ionic liquids are salts of an organic cation (e.g., ammonium, imidazolium, or phosphonium) and a counteranion (organic or inorganic) and, unlike mineral salts, are most often liquid at or near room temperature. This unique class of materials has been a topic of much research in the chemical sciences due to a range of remarkable properties including high electrical conductivity, excellent thermal stability, very low volatility, and good solvation capability for a broad range of organic, inorganic, and biological molecules. Such properties have motivated their use as alternative “green” reaction media for organic and enzymatic reactions.^{1,2} Apart from their use in chemical synthesis, ionic liquids (ILs) are of much interest as functional materials in electrochemical devices and batteries due to high electrical/ionic conductivity and wide voltage window.^{3–6} A key feature of molecular ionic liquids is that judicious selection of the anion and/or cation enables facile and predictive tailoring of properties such as viscosity, density, hydrophilicity/hydrophobicity, ionic conductivity, and chemical reactivity.^{7–9}

Such intriguing and tunable features of ILs have been introduced into solid materials either by physically doping ILs into bulk solids or in situ polymerization of monomers in ionic liquids to form “ionogels”,^{10–13} or by chemically linking ionic liquid molecules into polymeric matrices to yield “poly(ionic liquid)s” or PILs.^{14–16} In both cases, most of the salient

features of the ILs are retained and even coupled with the intrinsic properties of the original supporting materials. Furthermore, polymerization of ionic liquid monomers enables expanded functionality, increased chemical stability, and physical rigidity¹⁷ and also minimizes any material loss due to leaching.¹⁸ A number of recent studies have demonstrated applications of such novel hybrid materials in carbon dioxide capture, enzyme immobilization, and encapsulation for biocatalytic reactions and sensing,^{19,20} controlled drug delivery,²¹ lithium batteries, and electrochemical devices.²² The exquisite physicochemical tunability of these polymeric materials also makes them excellent candidates for the fabrication of smart stimuli-responsive gels for a broad range of potential applications.^{23–25} Of particular interest are anion-sensitive PILs, where the chemical nature of constituent anions dictates response of PILs to several features of their chemical environment.^{26–29} PILs are typically produced as bulk polymeric materials³⁰ and often lack regularity in size or shape.^{31–33} However, to realize their full potential, especially in applications involving portable, miniaturized environmental sensing and separations, it would be highly desirable to

Received: April 30, 2013

Revised: June 24, 2013

Published: June 27, 2013

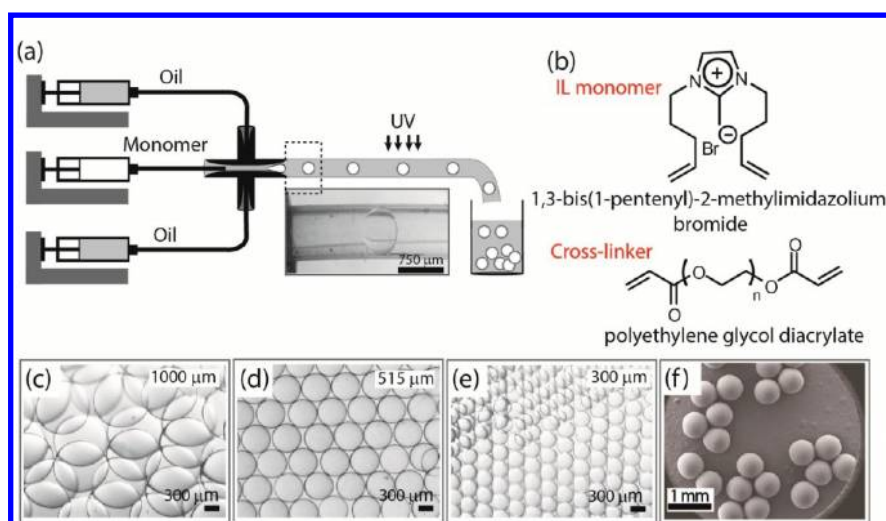


Figure 1. (a) Schematics illustrating capillary-based microfluidic method to generate poly (ionic liquid) microgels; inset shows a stereomicroscope image of a prepolymer droplet flowing in the transparent capillary tube. (b) Chemical structures of IL monomer and PEGDA cross-linker. (c–e) Stereomicroscope images of PIL microgels showing their monodispersity and transparency (average diameters of 1000, 515, and 300 μm , respectively). All scale bars are 300 μm . (f) FESEM image of synthesized PIL[Br]. Scale bar is 1 mm.

fabricate such materials with regular and tailored sizes and morphologies.

In this paper, we demonstrate simple, inexpensive microfluidics-based fabrication of highly monodisperse PIL microgels in particulate (bead) form with a multitude of functionalities that can be chemically switched in facile fashion by anion exchange and further enhanced by molecular inclusion. We show how the exquisite control over bead size and shape enables extremely precise, quantitative measurements of anion- and solvent-induced volume transitions in these materials, a crucial feature driving several important applications. Next, by exchanging diverse anions into the synthesized microgel beads, we demonstrate stimuli responsiveness and a multitude of functionalities including redox response, controlled release of chemical payloads, magnetization, toxic metal removal from water, and robust, *reversible* pH sensing.

EXPERIMENTAL SECTION

Ionic Liquid Monomer Synthesis. In a 500 mL round-bottom flask were taken 13.5 g (164 mmol) of 2-methylimidazole, 50.0 g (336 mmol, 2.0 equiv) of 5-bromo-1-pentene, and 55.0 g (400 mmol, 2.4 equiv) of potassium carbonate in 300 mL of acetonitrile. The mixture was vigorously stirred at 80 $^{\circ}\text{C}$ for 24 h. After cooling to room temperature, the mixture was filtered to remove all inorganic salts (excess potassium carbonate and byproduct potassium bromide). Then the filtrate was dried over magnesium sulfate to remove water and filtered again. This filtrate was dried in a rotary evaporator to remove all acetonitrile. A light yellow viscous ionic liquid was obtained which was washed with diethyl ether (each time 50 mL) to remove any unreacted starting materials. Finally, this ionic liquid monomer was dried in vacuum for extended time (24 h) to remove any trace of solvents. Yield of 1,3-bis(1-pentenyl)-2-methylimidazolium bromide ionic liquid monomer was 85%, based on 2-methylimidazole used.

Microfluidic Formation of PIL[Br] Microgels. We blended 1,3-bis(1-pentenyl)-2-methylimidazolium bromide ionic liquid monomer with aqueous PEGDA (poly(ethylene glycol) diacrylate, average M_n 700, Sigma-Aldrich) cross-linker and a photoinitiator (Darocur1173) in a ratio of IL monomer (65% w/w), PEGDA cross-linker (18% w/w), Darocur 1173 (7% w/w), and Milli-Q Water (10% w/w) to formulate the monomer fluid. We controllably generated aqueous drops of monomer liquid in an immiscible carrier fluid (silicone oil, 10 cst) inside a transparent microfluidic capillary reactor (Figure 1a), which

were subsequently polymerized by UV irradiation (365 nm, 15 W bulb). The tubing was wrapped around the UV lamp to accommodate longer residence time at high flow rates and to provide homogeneous UV exposure to the monomer droplets. We also used a small fan for cooling the UV-lamp to prevent any possible deformation of the tube due to heating. Individual syringe pumps (Harvard, PHD 2000) were used to deliver the carrier (silicone oil) and dispersed (monomer blend) liquids to a PEEK cross-junction. The sizes of the resultant polymeric microgel beads could be tuned by choosing the appropriate monomer and carrier fluid flow rates and the internal diameters of the capillary tube (diameter range of microbeads: 200–1000 μm). In all the applications presented in this paper, PIL microgels with average size of $517 \pm 15 \mu\text{m}$ (in hydrated state) were utilized. Silicone oil with a total flow rate of 50 $\mu\text{L}/\text{min}$ and monomer flow rate of 0.5 $\mu\text{L}/\text{min}$ were introduced to the PEEK cross-junction in order to achieve this size of microgels. The residence time for droplets of monomer blend in the UV-exposed environment was $\sim 120 \text{ s}$ (flow speed $\sim 0.003 \text{ m s}^{-1}$). During the continuous fabrication of PILs, the microbeads along with silicone oil were collected in a bottle. The as-synthesized microbeads were sequentially washed with hexane, ethanol, and water, for three times with each solvent assisted by $\sim 30 \text{ s}$ of vortex and 1 min of sonication at each step, to remove any residual silicone oil and starting reagents.

Characterization Methods. Structural characterization of synthesized IL monomer was carried out by ^1H and ^{13}C NMR (BRUKER, model AVANCE III 400) (Figure S1, Supporting Information (SI)). Synthesized PIL[Br] microgel beads were examined using CCD cameras (QImaging, MicroPublisher RTV 5.0 and Olympus, CAM-XC30) and stereomicroscopes (Olympus, SZX7 and 16SZ). A field emission scanning electron microscope (FESEM, JEOL 2011F) was used to determine the size and morphology of PIL materials. The complete polymerization and the presence of bromide and imidazolium group on the surface of PIL[Br] is supported by XPS, FTIR, elemental analysis, and EDX analyses. X-ray photoelectron spectroscopy (XPS) analysis was carried out on an Axis Ultra DLD (Kratos) spectrometer with Al mono $K\alpha$ X-ray source (1486.71 eV photons) to determine the elements. All binding energies (BEs) were referenced to the C 1s neutral carbon peak at 284.6 eV. In XPS measurements, C–C, C–O, and C–N bonds are identified along with the presence of bromide, suggesting the integration of imidazolium group and the counteranion into the polymeric material (Figure S2). Fourier transform infrared spectroscopy (FTIR) measurements were performed using a Perkin-Elmer spectrometer (model: Spectrum Two) with KBr as background over the range of 4000–400 cm^{-1} . Elemental analyses were performed on a Perkin-Elmer PE 2400

CHNS elemental analyzer. Energy-dispersive X-ray spectroscopy (EDX) analyses were carried out in an Oxford Instruments INCA system (15 kV) coupled with a JEOL 6500F field emission scanning electron microscope. Thermogravimetric analysis (TGA) was conducted on a TA Instruments analyzer (model: TA2050) to monitor the weight loss of dried PIL microgels and IL monomer under N_2 at temperatures from room temperature to $800\text{ }^\circ\text{C}$ at a rate of $5\text{ }^\circ\text{C}/\text{min}$ (Figure S3). FTIR, elemental analysis, and EDX were also used to support the presence of exchanged anions in PIL[X] microbeads (Figures S4, S5). Figure S5 also shows the presence of bromide in EDX analysis. The concentration of chromium in water was quantified by inductively coupled plasma mass spectrometry (ICP-MS, Agilent Technologies, ICP-MS, 7500 series). XPS analysis was also used to support the exchange of bromide with Cr(VI) in heavy metal removal experiment (section 6, SI).

RESULTS AND DISCUSSION

We employed a simple, robust droplet-based microfluidic method^{23,34} to fabricate highly monodisperse spherical PIL beads of varying average diameters in the submillimeter size range ($200\text{--}1000\text{ }\mu\text{m}$) for facile visual interrogation of their responses to various environmental stimuli (Figure 1).³⁵ We synthesized a doubly alkenylated imidazolium bromide ionic liquid as the IL-monomer (Figure 1b). This IL monomer has two symmetrical polymerizable groups, with the C-2 position of the imidazolium ring blocked with a methyl group to avoid any C-2 deprotonation in the processed polymer (Figure S1).³⁶ Additional advantages of this monomer included ease of preparation (see the SI for experimental details) and solubility in water. We tested two more ionic liquid monomers based on vinyl and acrylate functional groups respectively. 1-Methyl-3-vinyl imidazolium iodide is easy to prepare; however, only one polymerizable group (vinyl) is available in this case, and longer polymerization time is required ($>5\text{ min}$). Further, the materials obtained have low mechanical integrity and are difficult to handle for further treatment. Incorporating acrylate groups with imidazolium rings requires multiple steps while product quality is comparable to that from 1,3-bis(1-pentenyl)-2-methylimidazolium bromide. Moreover, in both vinyl and acrylate-based IL monomers, the C-2 positions are unprotected, which would be undesirable for several applications (e.g., heavy metal removal and recovery, pH sensing, and preparation of magnetic PIL beads) because transition metal ions are known to chemically attach to imidazolium rings via metal-imidazolium carbene-complex formation at the C-2 position. We selected poly(ethylene glycol) diacrylate (PEGDA) as a water-miscible cross-linker, which has been extensively used in polymeric microgels synthesis.²³ We optimized the compositions of the IL monomer, PEGDA, water, and photoinitiator (Darocur 1173) (65, 18, 10, and 7% w/w, respectively) in the prepolymer blend, such that the IL constituted the major component in the blend; sufficient PEGDA was present to promote rapid polymerization within typical microfluidic processing times ($\sim 2\text{ min}$), and phase separation of the water-immiscible photoinitiator was suppressed. Both carrier and dispersed fluids were continuously delivered into a PEEK cross-junction, using individual syringe pumps. We thereby controllably generated aqueous drops of polymer precursors in the immiscible carrier fluid (silicone oil) within a transparent microfluidic capillary reactor, which were subsequently polymerized by UV irradiation (Figure 1a). We obtained highly monodisperse PIL microgels at the exit of the reactor. The sizes of the resultant microgel beads could be tuned by choosing the appropriate monomer and external fluid flow rates and the internal diameters of the capillary tube

(Figure 1c–e).^{23,37,38} The as-synthesized microbeads were sequentially washed with hexane, ethanol, and water to remove any residual silicone oil or unreacted reagents. Microgel beads were of the same size in silicone oil, hexane and in the dried state while they swelled in ethanol and water; swollen PIL microbeads could revert back to the sizes of the first step when exposed to hexane or dried. The microbeads were sequentially and reversibly exposed to different solvents with a vacuum drying step between successive exposures, and it was found that the microbeads retained their respective sizes in that solvent or in the dried state. Hence, there was no discernible material loss due to washing. Chemical and physical characterization was carried out via several complementary techniques SEM (Figure 1f), EDX, XPS (Figures S2 and S5), and FTIR (Figure 2 and

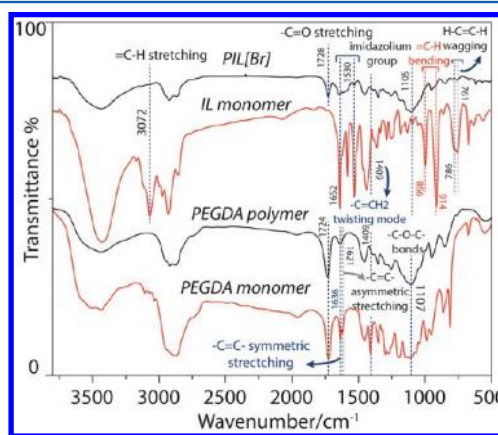


Figure 2. FTIR spectra of PEGDA monomer, PEGDA polymer, IL monomer, and poly(ionic liquid) PIL[Br].

Tables S1 and S2 in the SI). FTIR measurements indicated nearly complete attenuation of characteristic peaks due to monomer units (both from ionic liquid and PEGDA) in the polymer matrix (Figure 2), from which we inferred successful copolymerization of ionic liquid monomer with PEGDA. Elemental analysis of the hydrogel beads showed that the IL motif constitutes $\sim 60\%$ of the total mass of the bulk material, with $\sim 10\%$ of entrapped water and other volatiles as measured by thermogravimetric analysis (TGA). The presence of the constituent anion of PIL, in this case bromide, on the particle surface was validated via energy dispersive X-ray spectroscopy (EDX) analysis. The as-synthesized PIL microgels also showed high thermal stability of up to $230\text{ }^\circ\text{C}$ which is comparable to the parent ionic liquid monomer (Figure S3). Further characterization details are provided in the SI.

Anion-Dependent Volume Transitions. In the as-synthesized PILs, the imidazolium cations are fixed within the polymeric backbone while the bromide anions are labile. There is currently much interest in designing, understanding and exploiting the hydrogel volume transition in materials and biological applications.³⁹ In most studies, hydrogel volume transition in a particular environment is controlled by elaborate chemical optimizations: fine-tuning of composition (monomers and cross-linker), extent of cross-linking, electrolyte dopants, surfactants, and so forth. Clearly, the chemically and operationally simple procedure of labile anion exchange is a compelling alternative to tune hydrogel swelling or shrinkage. To accomplish this, we generated a diverse library of functional PIL beads by exchanging bromide with nine structurally and chemically diverse anions (chemical analyses validating anion

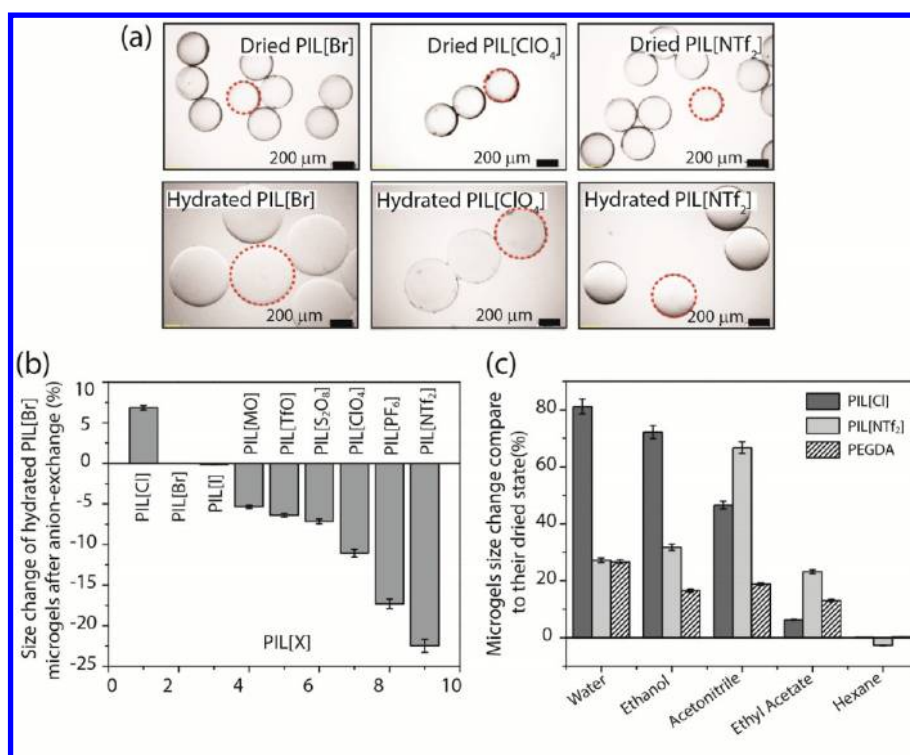


Figure 3. (a) Stereomicroscope images of samples of PIL[Br], PIL[ClO₄], and PIL[NTf₂] microgels with visibly similar sizes in the dried state and with distinct sizes in the hydrated state. All scale bars are 200 μm . (b) Plot of percentage size change (shrinkage/swelling) of hydrated PIL[Br] microgels after anion exchange with Cl⁻, I⁻, MO⁻, TfO⁻, (NH₄)₂S₂O₈²⁻, ClO₄⁻, PF₆⁻, and NTf₂⁻. (c) Plot of percentage size change of PIL[Cl], PIL[NTf₂] and PEGDA microgels (compared to the dried state) in various solvents. 50 microbeads were used for each measurement.

exchange are provided in the SI, Figures S4 and S5), and examined how each anion modified the size of parent PIL[Br] microgels under varying environments. Interestingly, for all anions tested, the dried beads had very similar sizes ($\sim 307 \pm 8 \mu\text{m}$) while large size variations (up to 38%) were observed in the hydrated state for different anions (Figure 3a,b). The microgel beads were highly monodisperse in all cases (CV < 3%, Figure S6). The trends in Figure 2b can be rationalized by analyzing the relative hydrophilicity/phobicity of the PILs in terms of their free IL counterparts. Though cations play a significant role in determining the physicochemical properties of ionic liquids, water content and relative hydrophilicity/phobicity are both principally dictated by the chemical nature of the anions.^{40–42} Anionic radii, charge density (partial charge), polarizability, and hydrogen-bond formation ability play significant roles in determining the extent of interaction and sorption of water in ILs. Differences in water sorption in molecular ionic liquids of up to 15% have been reported by varying the anions.⁴⁰ Halides are smaller than other polyatomic anions, possessing highly localized charge and hydrogen bonding capability; these features render PILs with halide anions most accommodating to water. In our case, the largest hydrogel diameter of PIL[Cl] microbeads can be attributed to the smallest size, high charge density, and greater hydration enthalpy of Cl among all halides used.⁴¹ Interestingly, identity of the constituent anion not only dictates the equilibrium diameter in the hydrated state, it also influences the time required for the attainment of swelling equilibrium. The hydration or swelling time for PIL microbeads presented in Figure 3b are 90 s for [Cl], 120 s for [Br], 135 s for [I], 150 s for [PF₆], 180 s for [ClO₄] and [NTf₂], and 225 s for [MO],

indicating that different anion–water interactions can regulate both the kinetic and thermodynamic outcome of swelling.

We further investigated the influence of anions in solvent-induced volume transitions, taking presumably the most hydrophilic (PIL[Cl]) and most hydrophobic (PIL[NTf₂]) microgel beads as model cases (Figure 3c). Both PIL[Cl] and PIL[NTf₂] assume similar sizes in solvent free conditions (dried state) or in highly nonpolar solvents such as hexane, while significant size differences (up to $\sim 80\%$) are observed in weakly and strongly polar (both protic and aprotic) solvents (Figure 3c). The diffuse nature of negative charge, lack of strong H-bonding, and lower hydration energy of PIL[NTf₂] imply comparatively less swelling in water and ethanol compared to PIL[Cl], in which the chloride anion can strongly interact via hydrogen bonding and dipole–dipole interactions.⁴³ Conversely, the nonpolar nature of ethyl acetate, a low dielectric solvent (dielectric constant ~ 6.02), implies that PIL[NTf₂] swells more than PIL[Cl].⁴⁴ Interestingly, although acetonitrile is highly polar (dielectric constant ~ 37.5), this aprotic solvent can interact with both the polar and nonpolar parts of ionic liquids which makes acetonitrile highly soluble particularly in NTf₂-based ILs.⁴⁵ Therefore, PIL[NTf₂] swells most in acetonitrile in our experiments, while the strong ion-pairing between imidazolium and chloride in PIL[Cl] presumably cannot be significantly perturbed by aprotic acetonitrile, thus resulting in less swelling compared to PIL[NTf₂]. It is noteworthy, when homopolymerized PEGDA microgels are exposed to various solvents (as above), swelling varies only between ~ 10 – 30% , attesting to the fact that the constituent ionic liquid (and associated anion) plays the major role in dictating the volume transition of PIL beads. In summary, the above results highlight how our monodisperse

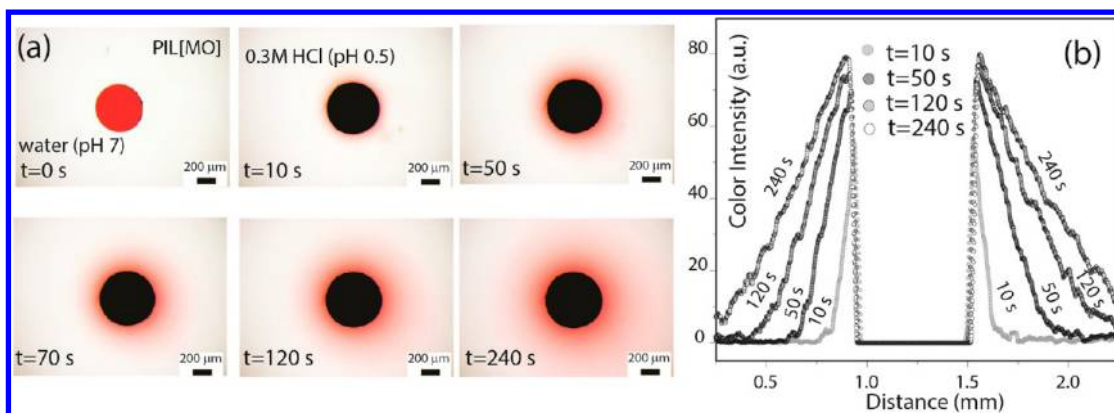


Figure 4. (a) Stereomicroscope images of PIL[MO] microbead at pH 7 and during controlled release of methyl orange from microbead to the surrounding medium at pH 0.5 (b) Measured diffusion profiles of MO from the PIL[MO] microbead to the surrounding environment. All scale bars are 200 μm .

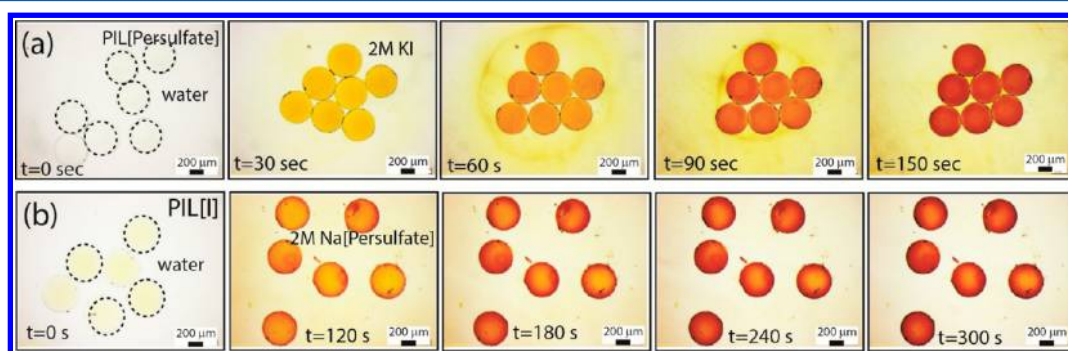


Figure 5. (a) Stereomicroscope images of reactive PIL microgels as "oxidizers"; PIL[S_2O_8] oxidizes iodide through the following reaction ($2\text{I}^- + \text{S}_2\text{O}_8^{2-} \rightarrow \text{I}_2 + 2\text{SO}_4^{2-}$). (b) Reactive PIL microgels, PIL[I], as "reducing" beads with persulfate anion in the solution-phase. All scale bars are 200 μm .

microgel beads enable precise measurements of anion-dependent volume transitions, which can be subsequently employed in a number of application scenarios.

Stimulus (pH)-Responsive Chemical Release. To demonstrate pH-responsive chemical release, we incorporated methyl orange (MO) by anion exchange of Br with MO (validation of anion exchange was done by elemental analysis, FTIR, and EDX of PIL[MO]; SI, Figures S4 and S5). We chose MO as a highly colored dye for facile visual inspection. When PIL[MO] beads were exposed to ultrapure water, no visible leaching of MO was observed, attesting the fact that MO was bound within the PIL via ion-pairing. However, when the pH of the surrounding aqueous medium was lowered (pH \sim 0.5) by adding HCl (pK_a of methyl orange is 3.47), slow sustained release of MO into water was observed (Figure 4a). After prolonged exposure (\sim 24 h) of the microbeads in HCl solution, they attained the original light yellow and transparent appearance, indicating complete release of the MO payload to the surrounding. EDX and elemental analysis of the obtained microgels showed complete absence of any residual sulfur (from MO or derivative). Prominent chloride peaks in EDX suggest that protonation of MO by HCl causes the slow release, where ion exchange between MO ion and chloride occurs to generate PIL[Cl]. The regular, symmetric bead shape enables quantitative measurement of MO diffusion kinetics into the surrounding medium, a valuable guide to understand the release profile for reactive molecules from such responsive materials. Figure 4b depicts measured diffusion profiles of MO from a PIL microgel bead to the surrounding environment at

various times; such profiles naturally suggest the possibility of measuring and understanding transport within and from the gel. For example, one can fit the release kinetics to simple diffusive transport models. However, we note that the profiles in Figure 4b are not amenable to a simple, analytical transport analysis, due to the nonideal geometry (sphere resting on a flat slab). A more "ideal" geometry would be to cast the gel as a flat slab and make similar measurements, as is common in hydrogel-based drug delivery. We therefore leave a more in-depth study to a separate communication, and suggest in summary that this system can be explored for similar pH-induced release of anionic drugs from the PIL matrix.²¹

Reactive PILs: Redox Reactions. Here we demonstrate the incorporation of redox active anions inside the PILs to perform chemical operations at the solid-solution boundaries of the microbeads. Recently, there has been growing interest in the synthesis and use of redox-active ionic liquids, either by simple ion exchange^{46,47} or covalent incorporation of redox-active groups onto the ionic liquid backbone;⁴⁸ however, to our knowledge, there is no report on the in situ modification of halide-based polymeric matrices into redox-active ones. We used PIL[Cl] as the base microbead to exchange Cl with an oxidizing (persulfate $\text{S}_2\text{O}_8^{2-}$) anion. After ion exchange, the molar ratio of Cl/sulfur in the resulting PIL[S_2O_8] microbeads was estimated from elemental analysis to be 1:11, implying that majority of chloride was exchanged with the redox active persulfate anion. When PIL[persulfate] beads were exposed to a 2 M solution of potassium iodide, immediate formation of molecular iodine (I_2) around the beads was observed,

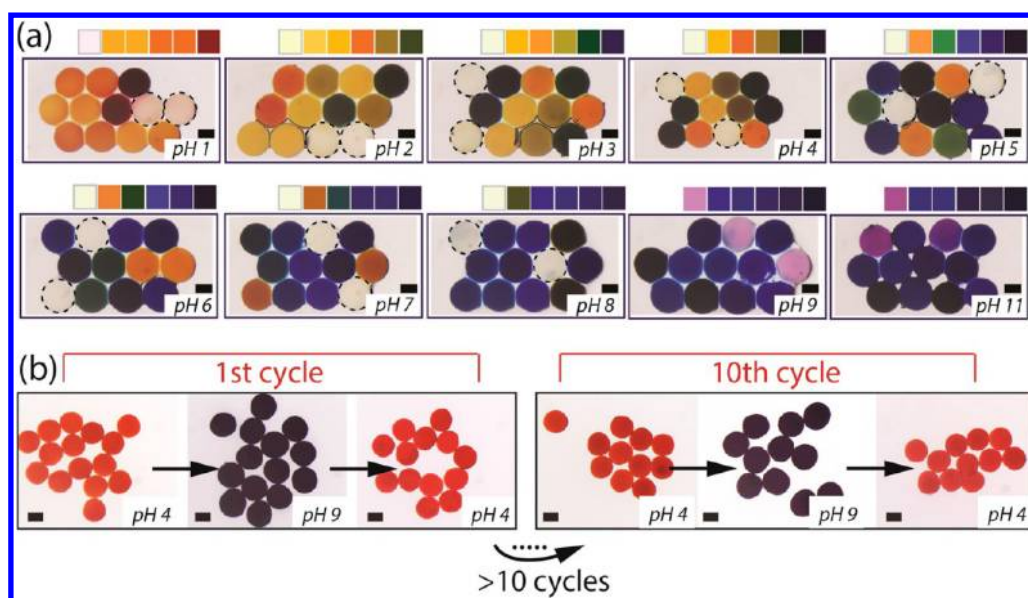


Figure 6. Reversible and recyclable pH-Strip with PIL microgels. (a) 3D pH Strip: an assortment of six pairs of different pH indicator-doped PIL microgels (two beads each contain the same pH indicator) are exposed to different pH solutions iteratively. (b) Reversible pH sensing: pH indicator (Thymol blue)-doped PIL microgels colorimetrically respond to the pH of the surrounding medium in a reversible fashion. The reversibility has been successfully tested for at least 10 cycles without any performance lost. All scale bars are 300 μm .

showcasing the capability of the entrapped oxidizing agent to perform a classical redox reaction (Figure 5a) ($2\text{I}^- + \text{S}_2\text{O}_8^{2-} \rightarrow \text{I}_2 + 2\text{SO}_4^{2-}$). To examine whether the persulfate anion leached out of the beads and then oxidized the iodide ions in the solution, we exposed PIL[persulfate] beads to water for ~ 12 h and tested the supernatant for its capability to oxidize potassium iodide. Expectedly, without the beads, no discernible iodine was detected in the aqueous supernatant by visual inspection, hence spontaneous leaching of persulfate from PIL beads in the absence of iodide can be assumed to be negligible. Complementarily, when PIL[I] was exposed to a 2 M $(\text{NH}_4)_2\text{S}_2\text{O}_8$ solution, immediate formation of iodine in the vicinity of PIL[I] surface showed that the redox active anions (persulfate and iodide) can react with each other, one in the polymer-bound state while the other as free aqueous anions (Figure 5b).

Chemical Separations: Heavy Metal Removal. Removal of chromium in the form of hexavalent chromium has been a major focus of wastewater purification techniques⁴⁹ and ion exchange based adsorbents are widely used for this purpose.^{50–52} The ability to rapidly exchange the parent bromide of as-synthesized PIL[Br] microgel beads with other anions, like toxic metal anions, can expand the application of these materials in separation and purification processes of toxic contaminants from water. In an appropriate pH-range (pH ~ 3), chromium(VI) remain as negatively charged anions, HCrO_4^- and $\text{Cr}_2\text{O}_7^{2-}$, that can be easily exchanged with bromide ions and hence the toxic metal components can be removed from the aquatic system by “ion-entrapment” (Figures S7 and S8). The as-synthesized PIL microgels are capable of reaching 74 mg/g adsorption capacity in chromium(VI) removal from wastewater, and the adsorption isotherm shows excellent agreement with the theoretical Langmuir isotherm (Figure S7). Equilibrium for chromium adsorption is reached within ~ 2 h. We briefly studied possible desorption routes to recover the adsorbed toxic metal ions from the PIL microbeads, which is essential for any potential regeneration of the adsorbent PIL microbeads. We found that dialysis of

chromate-doped beads with 0.01 M NaOH or 0.2 M phosphate buffer (Na_2HPO_4) enabled us to desorb 70% and 75% of the adsorbed chromate, respectively.

Magnetic PILs. Coordination, rather than direct exchange, of the halide anion of ILs with several metal salts can significantly modify the physicochemical nature of ionic liquids. For example, reaction of chloride-based ionic liquids IL[Cl] with FeCl_3 produces IL[FeCl_4] which is paramagnetic in nature.^{53,54} We tested a similar approach for our PIL[Cl] beads and incorporated FeCl_3 or DyCl_3 into the polymeric structure. A methanolic solution of FeCl_3 or DyCl_3 was added to dry PIL[Cl] beads to produce microgels that could be actuated with a simple hand-held magnet. Dy-based microgel beads were observed to be more magnetic than their Fe-based counterparts (a video is provided in the SI). This can be attributed to the greater effective magnetic moment of Dy ions ($\mu_{\text{eff}} = 10.4\text{--}10.6$ μB) compared to that of FeCl_4 ($\mu_{\text{eff}} = 5.8$ μB).⁵⁵

Chemical Sensing: pH. Finally, we demonstrate that PIL microgel beads can be used as solid-phase probes for robust and reversible pH sensing. Solid-phase immobilization of pH indicators is an active research area, particularly for pH measurements in biological systems. Such probes can non-invasively detect pH without chemical interference, thus being promising candidates for detection of, for example, extracellular pH gradients that are characteristics of tumor and wound environments and for investigation of the effect of pH on cellular migration.⁵⁵ Incorporation of pH indicator molecules into solid matrices typically requires chemical modification of both pH indicator and polymeric backbone^{56,57} or physical doping into a polymeric gel.^{58,59} As ionic liquids are known to accommodate several polar and nonpolar solute molecules, we opted to design PIL microgel-based pH sensors by stably doping small quantities of several commercially available pH indicators into the microbeads for reversibly probing a wide range of pHs, with minimum or no leaching of the indicator into aqueous analyte solution. We separately doped PIL[Br] microbeads with six different pH indicators to cover a wide range of pHs. Doping required less than 10 s, and no leaching

was observed after several washing steps. When each category of PIL-indicator beads was exposed to solutions with varying pH, distinct colors were observed within the beads with negligible indicator leaching (A matrix of images for individual indicators is provided in SI, Figure S9). We constructed a simple bead-based pH-strip with an assortment of six pairs of different indicator-doped microgel beads (Figure 6). Upon exposure to different pH environments these beads assumed a distinct, uniquely pH-dependent band of colors, very much analogous to commercial pH-strips (Figure 6a). An elegant and unique feature of these pH-indicator microgel beads is that they respond reversibly to the switching of pH environments. As shown in Figure 6b, Thymol blue-doped PIL microgels can be switched between pHs 4 and 9 ten times without any leaching or compromised performance (in terms of color intensity and response time). Such reversible, reusable, and noninvasive pH sensing, unlike the conventional method of doping soluble pH indicator into the analyte solution, may pave the way for monitoring biological or other sensitive samples where cross-contamination by the indicator itself could be detrimental. Stable confinement of the indicator dye molecules within the PIL matrix can be attributed to electrostatic interactions between the ionizable indicator molecules and imidazolium groups, as well as to the hydrophobic interaction of alkyl ($-\text{CH}_2-$ groups) side chains of the ionic liquid segments with the nonpolar moieties (alkyl and aromatic) of the indicators.⁶⁰ Such interactions are not present within PEGDA microbeads, thus explaining the differences in indicator retention from the PIL[Br] beads. During indicator doping, PIL microgel beads show visible, nearly instantaneous (approx. seconds) color change when exposed to indicator solutions, and the indicator is retained stably (at pH 7) within the beads over several months. In contrast, PEGDA microbeads do not show a distinct color change even after hours of exposure to indicator solution, and the indicators leach out while stored in neutral water (within ~ 24 h). Moreover, upon exposing indicator-doped PIL microbeads to a solution of controlled pH in a small microwell, mild pipette tip-aided stirring results in rapid response of PILs to the surrounding pH (seconds to minutes), while PEGDA beads respond to pH change on a time scale of minutes to hours under similar conditions. Specific response times vary within these ranges, depending on the indicator used and pH level. Response time for such sensing can be very crucial should these beads be used in flow-cell based sensing devices. Thus, we believe the ionic liquid motif is essential for the stable doping and quick and reversible sensing of the pH. Further along similar lines, we also demonstrate a capillary-based 3D pH-strip for iterative pH analyses, where PIL microgels are embedded inside a glass-capillary and are exposed to flowing solutions with varying pH (Figure S10).

CONCLUSIONS

In conclusion, we employ a simple and inexpensive microfluidic method to fabricate monodisperse spherical polymeric ionic liquid microgel beads. We demonstrate how simple anion exchange can enable fine-tuning of size and swellability of these beads. By incorporating diverse anions, we are able to impart a multitude of functionalities to these beads, ranging from redox-capabilities, controlled-release of payload, magnetization, toxic metal removal and robust, reversible pH sensing. We envision that these chemically switchable stimulus-responsive beads will open up a vast array of potential applications in portable and preparative chemical analysis, separations and spatially

addressed sensing. They can, for example, be geometrically arrayed as 1D or 2D matrices to perform cascades of chemical reactions, separation, and sensing in integrated, flow-through fashion by judiciously choosing the anions for each operation.

ASSOCIATED CONTENT

Supporting Information

Full description of materials used, experimental details and characterization results of synthesized IL monomer; microfluidic formation of PIL[Br] and PEGDA microgels; anion-dependent volume transitions; stimulus (pH)-responsive chemical release; reactive PILs- redox reactions; chemical separations, heavy metal removal; magnetic PILs, chemical sensing, pH. This material is available free of charge via the Internet at <http://pubs.acs.org>.

AUTHOR INFORMATION

Corresponding Author

*E-mail: saifkhan@nus.edu.sg.

Author Contributions

[†]M.T.R. and Z.B. contributed equally to this work.

Notes

The authors declare no competing financial interest.

ACKNOWLEDGMENTS

The authors thank Dominik Jarde for help with the initial experiments and optimization of polymerization conditions, and Prof. Ilhyong Ryu and Prof. Takahide Fukuyama (Department of Chemistry, Osaka Prefecture University, Japan) for generously providing us with the UV lamp. The authors gratefully acknowledge research funding from Singapore-MIT Alliance (CPE program): Flagship Research Project (FRP) and Inter-University Project (IUP) initiatives. P.S.D. acknowledges partial support from the Singapore-MIT International Design Centre.

REFERENCES

- (1) Hallett, J. P.; Welton, T. Room-Temperature Ionic Liquids: Solvents for Synthesis and Catalysis. 2. *Chem. Rev.* **2011**, *111*, 3508–3576.
- (2) van Rantwijk, F.; Sheldon, R. A. Biocatalysis in Ionic Liquids. *Chem. Rev.* **2007**, *107*, 2757–2785.
- (3) Chum, H. L.; Koch, V. R.; Miller, L. L.; Osteryoung, R. A. Electrochemical Scrutiny of Organometallic Iron Complexes and Hexamethylbenzene in a Room Temperature Molten Salt. *J. Am. Chem. Soc.* **1975**, *97*, 3264–3265.
- (4) Armand, M.; Endres, F.; MacFarlane, D. R.; Ohno, H.; Scrosati, B. Ionic-liquid Materials for the Electrochemical Challenges of the Future. *Nat. Mater.* **2009**, *8*, 621–629.
- (5) MacFarlane, D. R.; Forsyth, M.; Howlett, P. C.; Pringle, J. M.; Sun, J.; Annat, G.; Neil, W.; Izgorodina, E. I. Ionic Liquids in Electrochemical Devices and Processes: Managing Interfacial Electrochemistry. *Acc. Chem. Res.* **2007**, *40*, 1165–1173.
- (6) Hapiot, P.; Lagrost, C. Electrochemical Reactivity in Room-Temperature Ionic Liquids. *Chem. Rev.* **2008**, *108*, 2238–2264.
- (7) Ohno, H. Functional Design of Ionic Liquids. *Bull. Chem. Soc. Jpn.* **2006**, *79*, 1665–1680.
- (8) Hardacre, C.; Holbrey, J. D.; Nieuwenhuyzen, M.; Youngs, T. G. A. Structure and Solvation in Ionic Liquids. *Acc. Chem. Res.* **2007**, *40*, 1146–1155.
- (9) Chiappe, C.; Pieraccini, D. Ionic liquids: Solvent Properties and Organic Reactivity. *J. Phys. Org. Chem.* **2005**, *18*, 275–297.
- (10) Le Bideau, J.; Viau, L.; Vioux, A. Ionogels, Ionic Liquid Based Hybrid Materials. *Chem. Soc. Rev.* **2011**, *40*, 907–925.

- (11) Néouze, M.-A.; Bideau, J. L.; Gaveau, P.; Bellayer, S.; Vioux, A. Ionogels, New Materials Arising from the Confinement of Ionic Liquids within Silica-Derived Networks. *Chem. Mater.* **2006**, *18*, 3931–3936.
- (12) Vioux, A.; Viau, L.; Volland, S.; Le Bideau, J. Use of Ionic Liquids in Sol-gel; Ionogels and Applications. *C.R. Chim.* **2010**, *13*, 242–255.
- (13) Kavanagh, A.; Byrne, R.; Diamond, D.; Fraser, K. J. Stimuli Responsive Ionogels for Sensing Applications—An Overview. *Membranes* **2012**, *2*, 16–39.
- (14) Lu, J.; Yan, F.; Texter, J. Advanced Applications of Ionic Liquids in Polymer Science. *Prog. Polym. Sci.* **2009**, *34*, 431–448.
- (15) Mecerreyes, D. Polymeric ionic liquids: Broadening the Properties and Applications of Polyelectrolytes. *Prog. Polym. Sci.* **2011**, *36*, 1629–1648.
- (16) Yuan, J. Y.; Antonietti, M. Poly(ionic liquid)s: Polymers Expanding Classical Property Profiles. *Polymer* **2011**, *52*, 1469–1482.
- (17) Green, O.; Grubjesic, S.; Lee, S.; Firestone, M. A. The Design of Polymeric Ionic Liquids for the Preparation of Functional Materials. *Polym. Rev.* **2009**, *49*, 339–360.
- (18) Chen, H.; Choi, J.-H.; Salas-de la Cruz, D.; Winey, K. I.; Elabd, Y. A. Polymerized Ionic Liquids: The Effect of Random Copolymer Composition on Ion Conduction. *Macromolecules* **2009**, *42*, 4809–4816.
- (19) Nakashima, K.; Kamiya, N.; Koda, D.; Maruyama, T.; Goto, M. Enzyme Encapsulation in Microparticles Composed of Polymerized Ionic Liquids for Highly Active and Reusable Biocatalysts. *Org. Biomol. Chem.* **2009**, *7*, 2353–2358.
- (20) López, M.; Mecerreyes, D.; López-Cabarcos, E.; López-Ruiz, B. Amperometric Glucose Biosensor Based on Polymerized Ionic Liquid Microparticles. *Biosens. Bioelectron.* **2006**, *21*, 2320–2328.
- (21) Cui, W.; Lu, X.; Cui, K.; Niu, L.; Wei, Y.; Lu, Q. Dual-Responsive Controlled Drug Delivery Based on Ionically Assembled Nanoparticles. *Langmuir* **2012**, *28*, 9413–9420.
- (22) Xiong, Y.-B.; Wang, H.; Wang, Y.-J.; Wang, R.-M. Novel Imidazolium-based Poly(ionic liquid)s: Preparation, Characterization, and Absorption of CO₂. *Polym. Adv. Technol.* **2012**, *23*, 835–840.
- (23) Dendukuri, D.; Doyle, P. S. The Synthesis and Assembly of Polymeric Microparticles Using Microfluidics. *Adv. Mater.* **2009**, *21*, 4071–4086.
- (24) Hwang, D. K.; Oakey, J.; Toner, M.; Arthur, J. A.; Anseth, K. S.; Lee, S.; Zeiger, A.; Van Vliet, K. J.; Doyle, P. S. Stop-Flow Lithography for the Production of Shape-Evolving Degradable Microgel Particles. *J. Am. Chem. Soc.* **2009**, *131*, 4499–4504.
- (25) Seiffert, S.; Weitz, D. A. Microfluidic Fabrication of Smart Microgels from Macromolecular Precursors. *Polymer* **2010**, *51*, 5883–5889.
- (26) Batra, D.; Hay, Firestone, M. A. Formation of a Biomimetic, Liquid-Crystalline Hydrogel by Self-Assembly and Polymerization of an Ionic Liquid. *Chem. Mater.* **2007**, *19*, 4423–4431.
- (27) Suarez, I. J.; Sierra-Martin, B.; Fernandez-Barbero, A. Swelling of Ionic and Non-Ionic Minigels. *Colloids Surf., A* **2009**, *343*, 30–33.
- (28) Texter, J. Anion Responsive Imidazolium-Based Polymers. *Macromol. Rapid Commun.* **2012**, *33*, 1996–2014.
- (29) Suárez, I. n. J.; Rubio-Retama, J.; Sierra-Martín, B. n.; Javier de las Nieves, F.; Mecerreyes, D.; López-Cabarcos, E.; Márquez, M.; Fernández-Barbero, A. Ion-Specific and Reversible Wetting of Imidazolium-Based Minigels. *J. Phys. Chem. B* **2008**, *112*, 10815–10820.
- (30) Tokuda, M.; Minami, H.; Mizuta, Y.; Yamagami, T. Preparation of Micron-Sized Monodisperse Poly(ionic liquid) Particles. *Macromol. Rapid Commun.* **2012**, *33*, 1130–1134.
- (31) Muldoon, M. J.; Gordon, C. M. Synthesis of Gel-Type Polymer Beads from Ionic Liquid Monomers. *J. Polym. Sci., Part A: Polym. Chem.* **2004**, *42*, 3865–3869.
- (32) Yuan, J.; Antonietti, M. Poly(ionic liquid) Latexes Prepared by Dispersion Polymerization of Ionic Liquid Monomers. *Macromolecules* **2011**, *44*, 744–750.
- (33) Marcilla, R.; Sanchez-Paniagua, M.; Lopez-Ruiz, B.; Lopez-Cabarcos, E.; Ochoteco, E.; Grande, H.; Mecerreyes, D. Synthesis and Characterization of New Polymeric Ionic Liquid Microgels. *J. Polym. Sci., Part A: Polym. Chem.* **2006**, *44*, 3958–3965.
- (34) Tumarkin, E.; Kumacheva, E. Microfluidic Generation of Microgels from Synthetic and Natural Polymers. *Chem. Soc. Rev.* **2009**, *38*, 2161–2168.
- (35) Barikbin, Z.; Rahman, M. T.; Jardeh, D.; Badruddoza, M. A. Z.; Doyle, S. P.; Khan, S. A. Microfluidic Fabrication of Polymerized Ionic Liquid Microgels. In *Proceedings of μTAS*; Okinawa, Japan, 2012; pp 1786–1788.
- (36) Sowmiah, S.; Srinivasadesikan, V.; Tseng, M.-C.; Chu, Y.-H. On the Chemical Stabilities of Ionic Liquids. *Molecules* **2009**, *14*, 3780–3813.
- (37) Kumacheva, E.; Garstecki, P. In *Microfluidic Reactors for Polymer Particles*; John Wiley & Sons, Ltd: Chichester, UK, 2011; Ch. 8.
- (38) Wang, J.-T.; Wang, J.; Han, J.-J. Fabrication of Advanced Particles and Particle-Based Materials Assisted by Droplet-Based Microfluidics. *Small* **2011**, *7*, 1728–1754.
- (39) Wu, S.; Li, H.; Chen, J. P.; Lam, K. Y. Modeling Investigation of Hydrogel Volume Transition. *Macromol. Theory Simul.* **2004**, *13*, 13–29.
- (40) Cao, Y.; Chen, Y.; Sun, X.; Zhang, Z.; Mu, T. Water Sorption in Ionic Liquids: Kinetics, Mechanisms and Hydrophilicity. *Phys. Chem. Chem. Phys.* **2012**, *14*, 12252–12262.
- (41) Klähn, M.; Stüber, C.; Seduraman, A.; Wu, P. What Determines the Miscibility of Ionic Liquids with Water? Identification of the Underlying Factors to Enable a Straightforward Prediction. *J. Phys. Chem. B* **2010**, *114*, 2856–2868.
- (42) Cammarata, L.; Kazarian, S. G.; Salter, P. A.; Welton, T. Molecular States of Water in Room Temperature Ionic Liquids. *Phys. Chem. Chem. Phys.* **2001**, *3*, 5192–5200.
- (43) Chiappe, C.; Malvaldi, M.; Pomelli, C. S. Ionic Liquids: Solvation Ability and Polarity. *Pure Appl. Chem.* **2009**, *81*, 767–776.
- (44) Bonhote, P.; Dias, A.-P.; Papageorgiou, N.; Kalyanasundaram, K.; Grätzel, M. Hydrophobic, Highly Conductive Ambient-Temperature Molten Salts. *Inorg. Chem.* **1996**, *35*, 1168–1178.
- (45) Bardak, F.; Xiao, D.; Hines, L. G.; Son, P.; Bartsch, R. A.; Quitevis, E. L.; Yang, P.; Voth, G. A. Nanostructural Organization in Acetonitrile/Ionic Liquid Mixtures: Molecular Dynamics Simulations and Optical Kerr Effect Spectroscopy. *ChemPhysChem* **2012**, *13*, 1687–1700.
- (46) Cho, S. D.; Im, J. K.; Kim, H.-K.; Kim, H. S.; Park, H. S. Functionalization of Reduced Graphene Oxides by Redox-Active Ionic Liquids for Energy Storage. *Chem. Commun.* **2012**, *48*, 6381–6383.
- (47) Mariani, A.; Nuvoli, D.; Alzari, V.; Pini, M. Phosphonium-Based Ionic Liquids as a New Class of Radical Initiators and Their Use in Gas-Free Frontal Polymerization. *Macromolecules* **2008**, *41*, 5191–5196.
- (48) Sui, X.; Hempenius, M. A.; Vancso, G. J. Redox-Active Cross-Linkable Poly(ionic liquid)s. *J. Am. Chem. Soc.* **2012**, *134*, 4023–4025.
- (49) Hu, J.; Chen, G.; Lo, I. M. C. Removal And Recovery of Cr(VI) from Wastewater by Maghemite Nanoparticles. *Water Res.* **2005**, *39*, 4528–4536.
- (50) Cao, C.-Y.; Qu, J.; Yan, W.-S.; Zhu, J.-F.; Wu, Z.-Y.; Song, W.-G. Low-Cost Synthesis of Flowerlike α-Fe₂O₃ Nanostructures for Heavy Metal Ion Removal: Adsorption Property and Mechanism. *Langmuir* **2012**, *28*, 4573–4579.
- (51) Abou El-Reash, Y. G.; Otto, M.; Kenawy, I. M.; Ouf, A. M. Adsorption of Cr(VI) and As(V) Ions by Modified Magnetic Chitosan Chelating Resin. *Int. J. Biol. Macromol.* **2011**, *49*, 513–522.
- (52) Deng, Y.; Long, T.; Zhao, H.; Zhu, L.; Chen, J. Application of Porous N-Methylimidazolium Strongly Basic Anion Exchange Resins on Cr(VI) Adsorption from Electroplating Wastewater. *Sep. Sci. Technol.* **2011**, *47*, 256–263.
- (53) Yoshida, Y.; Saito, G. Design of Functional Ionic Liquids Using Magneto- and Luminescent-Active Anions. *Phys. Chem. Chem. Phys.* **2010**, *12*, 1675–1684.

(54) Dobbelin, M.; Jovanovski, V.; Llarena, I.; Claros Marfil, L. J.; Cabanero, G.; Rodriguez, J.; Mecerreyes, D. Synthesis of Paramagnetic Polymers Using Ionic Liquid Chemistry. *Polym. Chem.* **2011**, *2*, 1275–1278.

(55) Paradise, R. K.; Whitfield, M. J.; Lauffenburger, D. A.; Van Vliet, K. J. Directional Cell Migration in an Extracellular pH Gradient: A Model Study With an Engineered Cell Line and Primary Microvascular Endothelial Cells. *Exp. Cell Res.* **2013**, *319*, 487–497.

(56) Li, G.; Xiao, J.; Zhang, W. A Novel Dual Colorimetric Fiber Based on Two Acid-Base Indicators. *Dyes Pigm.* **2012**, *92*, 1091–1099.

(57) Czugala, M.; Gorkin Iii, R.; Phelan, T.; Gaughran, J.; Curto, V. F.; Ducree, J.; Diamond, D.; Benito-Lopez, F. Optical Sensing System Based on Wireless Paired Emitter Detector Diode Device and Ionogels for Lab-on-a-Disc Water Quality Analysis. *Lab Chip* **2012**, *12*, 5069–5078.

(58) Maruyama, H.; Arai, F.; Fukuda, T. On-Chip pH Measurement Using Functionalized Gel-Microbeads Positioned by Optical Tweezers. *Lab Chip* **2008**, *8*, 346–351.

(59) Beebe, D. J.; Moore, J. S.; Yu, Q.; Liu, R. H.; Kraft, M. L.; Jo, B.-H.; Devadoss, C. Microfluidic Tectonics: A Comprehensive Construction Platform for Microfluidic Systems. *Proc. Natl. Acad. Sci. U.S.A.* **2000**, *97*, 13488–13493.

(60) Pei, Y. C.; Wang, J. J.; Xuan, X. P.; Fan, J.; Fan, M. Factors Affecting Ionic Liquids Based Removal of Anionic Dyes from Water. *Environ. Sci. Technol.* **2007**, *41*, 5090–5095.